# Thermal and Mechanical Properties of Poly(ethylene terephthalate)/Lamellar Zirconium Phosphate Nanocomposites

**Lilian S. Brandão,[1] Luís C. Mendes,[1] Marta E. Medeiros,[2] Lys Sirelli,[1] Marcos L. Dias[1]**

[1]*Instituto de Macromoléculas Professora Eloisa Mano, Universidade Federal do Rio de Janeiro, CP 68525, Rio de Janeiro 21945-970, Brazil*
[2]*Departamento de Química Inorgânica, Instituto de Química, Universidade Federal do Rio de Janeiro, CP 68563, Rio de Janeiro 21945-970, Brazil*

Received 17 June 2005; accepted 29 December 2005
DOI 10.1002/app.24096
Published online in Wiley InterScience (www.interscience.wiley.com).

**ABSTRACT:** The preparation of nanocomposites of poly (ethylene terephthalate) (PET) and lamellar zirconium phosphorous compounds by melt extrusion was investigated. Two types of zirconium phosphorous compounds were synthesized by the direct precipitation reaction method: α-zirconium bis(monohydrogen orthophosphate) monohydrate (ZrP) and organic–inorganic hybrid layered zirconium phenylphosphonate (ZrPP). Composites containing 2 and 5 wt % ZrP and ZrPP were prepared in a twin-screw extruder and specimens were obtained by injection molding. The extent of dispersion of the layered filler in the composite matrix was investigated by X-ray diffraction and transmission electron microscopy (TEM). The crystallization and thermal properties were analyzed by differential scanning calorimetry and thermogravimetry, and the mechanical properties were evaluated by tensile tests. Whereas ZrP-containing composites showe characteristic diffraction peaks at 2θ 11.7° ($d$ = 7.54 Å), indicative of no delamination, ZrPP showed practically no low-angle diffraction peak at 2θ 5.5° ($d$ = 15.24 Å), indicating loss of the layered order. TEM images of ZrPP particles indicated the formation of an intercalated/partially delaminated nanocomposite. The behavior was attributed to the higher affinity of the polyester with phenyl groups on the platelet surface of ZrPP. In both cases, the addition of the fillers increased the crystallization rate and the modulus. © 2006 Wiley Periodicals, Inc. J Appl Polym Sci 102: 3868–3876, 2006

**Key words:** poly(ethylene terephthalate); nanocomposites; zirconium phosphate; zirconium phenylphosphonate

## INTRODUCTION

Organic–inorganic nanoscaled composites comprise an important class of synthetic engineering materials. Their structures are such that they can be transformed into new materials with the advantages of both organic materials, such as light weight, flexibility, and good molding, and inorganic materials, like high strength, heat stability, and chemical resistance.[1] Organic–inorganic nanocomposites can result in materials with excellent stiffness, strength, and gas barrier properties with far less inorganic content than is used in conventionally filled polymer composites.[2] Their rigidity, mechanical strength, and barrier properties are improved while simultaneously maintaining the same transparency level and high elongation of the base polymer.[3]

Layered particles can be used as reinforcing fillers in their aggregated form, but they can be much more effective when the lamellae layers are exfoliated.[4]

Nanocomposites based on layered nanofillers can be prepared by polymer intercalation from solution, *in situ* polymerization (intercalation of a monomer followed by polymerization), or melt intercalation (interaction of the polymer in the melt state).[4] Depending on the process used (and its conditions) and the interactions between the polymer and the layers, two different kinds of nanocomposites can be formed: intercalated and exfoliated. Intercalated nanocomposites consist of regular insertion of polymer in between the layers and exfoliated nanocomposites are constituted of 1-nm thickness layers dispersed in the polymer matrix, forming a microscale monolithic structure.

The extensive diversity of lamellar materials found in nature like clay (aluminum silicate), halides of transition metals, hydroxides of bivalent metals, and phosphates of tetravalent metals can be used in nanocomposite production.[5] There have been successful examples of polymer/inorganic nanocomposites reported, from which one of the most active research fields has developed into a new materials field called polymers/layered clay nanocomposites. The most commonly used clay in polymer nanocomposites is montmorillonite, which is obtained from bentonite.

*Correspondence to:* M. L. Dias (mldias@ima.ufrj.br).
Contract grant sponsors: CNP, FAPERJ.

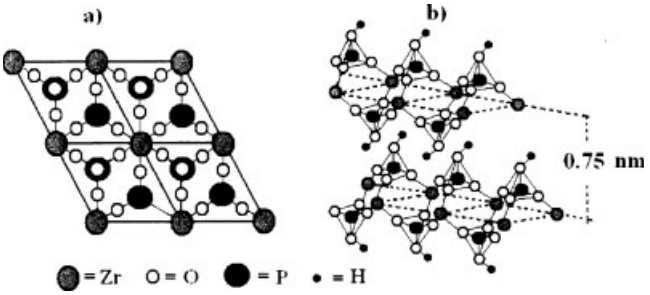


**Figure 1** The structure of α-ZrP: (a) plane and (b) tridimensional.

Phosphates of tetravalent metals have the general formula $M(HPO_4)_2 \cdot nH_2O$, where M is a tetravalent metal, such as Ti, Zr, Hf, Ge, Sn, Pb, or Th.[6]

Zirconium bis(monohydrogen orthophosphate) monohydrate, with the formula $\alpha$-$Zr(HPO_4)_2 \cdot H_2O$ ($\alpha$-ZrP), is a crystalline material with many interesting features, such as ion-exchange properties, thermal and chemical stability,[6] catalytic activity, ionic conductivity, and intercalation properties.[7] Many of these properties are common to natural layered fillers such as montmorollonite. Nevertheless, in contrast to this clay, α-ZrP has acid groups on the internal surface of the layers, allowing direct intercalation of a variety of substances, especially basic compounds such as alkylamines.[8]

α-ZrP has a layered structure in which the metal atoms lie nearly in a plane and are bridged by phosphate groups. Three oxygen atoms of each phosphate are bonded to three different zirconium atoms arranged at the apices of a near equilateral triangle [Fig. 1(a)]. The fourth bond passes from the layer and bonds a hydrogen atom. Adjacent layers are staggered in a pseudohexagonal manner so as to form six-sided cavities between the layers [Fig. 1(b)]. A water molecule is set in the center of each cavity. The α-ZrP crystal has an interlayer distance of 7.56 Å.[6]

Another fundamental step in the development of the chemistry of α-layered materials was the 1978 discovery that compounds of the type $Zr(RPO_3)_2$ and $Zr(ROPO_3)_2$ (where R = organic radical) with lamellar α-type structures can be prepared by simply replacing $H_3PO_4$ with the acids $RPO_3H_2$ or $ROPO_3H_2$ in the synthesis of α-ZrP.[9]

As an example, consider the matrix interlayer distance of 15 Å for $Zr(C_6H_5PO_3)_2$, in which the opposite sides of each layer contain phenyl rings with individual lengths of 5.85 Å.[10] Figure 2 shows a representation of zirconium phenylphosphonate and α-ZrP layers. A free interlayer space of 3.3 Å remained from this proposed arrangement. Considering the structure of these organic–inorganic hybrid layered phosphates, it is expected that a polymer with affinity with the surface of the organic-modified lamellae could be capable of entering inside the channels, exfoliating the phosphate.

In this work, the effect of the addition of different percentages of zirconium bis(monohydrogen orthophosphate), with the formula $Zr(HPO_4)_2 \cdot H_2O$ (ZrP), and zirconium phenylphosphonate, with the formula $Zr(C_6H_5PO_3)_2$ (ZrPP), on the mechanical and thermal properties of poly(ethylene terephthalate) (PET) was investigated. We report the first successful attempt to prepare a PET nanocomposite with zirconium phenylphosphonate.

## EXPERIMENTAL

### Materials

Bottle-grade PET (intrinsic viscosity = 0.78 dL/g, Brasken) was used in this work. The layered zirconium compounds were synthesized as described below.

### Synthesis of layered zirconium compounds

ZrP was prepared by the direct precipitation reaction method.[11] A mixture of phosphoric acid ($H_3PO_4$, Synth) and zirconium(IV) oxide chloride 8-hydrate ($ZrOCl_2 \cdot 8H_2O$, Vetec) in a [P/Zr] ratio of 2.5 was maintained under reflux for 48 h. Precipitated crystals were separated by filtration, washed with distilled water to a pH of ~ 4, and dried at room temperature.

ZrPP was synthesized by refluxing a mixture of phenyl phosphonic acid ($C_6H_5PO_3H_2$, Aldrich) and $ZrOCl_2 \cdot 8H_2O$ (Vetec, Brazil) in a [P/Zr] ratio of 2.5 for 24 h. Precipitated crystals were separated by filtration, washed with distilled water to a pH of ~ 4, and dried at room temperature.[9,12]

### Composite preparation

PET (pellets) and crystals of ZrP or ZrPP were mixed in a Haake counterrotating twin-screw extruder at 280°C and a screw speed of 90 rpm. Each composition was processed twice as above to improve homogeneity. Two different compositions were prepared: 2 and 5 wt % ZrP or ZrPP. Extruded composites were pellet-

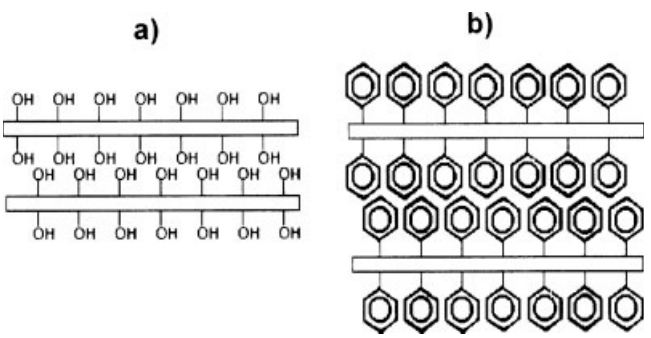


**Figure 2** Representations of (a) ZrP and (b) ZrPP layers.

ized, dried at 165°C for 16 h, and then injection molded into standard specimens (ISO 527) in a Ray Ran injection molding machine using a barrel temperature of 285°C, a mold temperature of 40°C (30 s), and an injection pressure of 8 bar. The PET pellets were dried in an oven at 165°C for 16 h before processing.

### Composite characterization

Small- and wide-angle X-ray diffraction (XRD) experiments were performed on specimens using a Rigaku Miniflex diffractometer with Cu Kα radiation (λ = 1.5418 Å). The generator was operated at 30 kV and 20 mA. Samples were scanned from 2θ 2.0–35° at a scanning rate of 1°/min. Layer spacing ($d$) was calculated by using the Bragg relation, $\lambda = 2d \sin\theta$, considering the lower 2θ reflexion related to the plane *hkl* 002.

Ultrathin sections of the composites with a thickness of approximately 50 nm were prepared in a Reichert ultramicrotome Ultracut S50 equipped with a diamond knife. Transmission electron microscopy (TEM) was carried out in JEOL TEM-1210 equipment using an accelerator voltage of 60 kV. Staining of the samples was not used because of the high electron density difference between PET and the zirconium compounds.

The thermal properties were measured using a differential scanning calorimetry (DSC) PerkinElmer DSC-7 calorimeter. Each sample was heated from 40 to 300°C at a scanning rate of 10°C/min, kept at this temperature for 2 min, and cooled to 30°C at a scanning rate of 10°C/min. A second heating procedure was then performed to 300°C at the same scanning rate. The melting temperature ($T_m$) was considered to be the maximum of the endothermic melting peak and the crystallization temperatures of the exothermic peak of the crystallization from heating ($T_{ch}$) and cooling ($T_{cc}$) scans. The degree of crystallinity ($X_c$) was calculated from the ratio of the melting endotherm ($\Delta H_m$) and the melt enthalpy of 100% crystalline PET, considered as 136 J/g.[13] The degree of crystallinity of the specimens was calculated taking into consideration the enthalpy of crystallization on heating ($\Delta H_{cc}$).

Thermogravimetry was used to evaluate the thermal stability of the samples. The analyses were carried out in a PerkinElmer TGA7 from 50 to 700°C at 10°C/min under nitrogen.

The mechanical properties (stress–strain) were measured according to the ISO 527 method in an Instron model 4204 tensile testing machine at a rate of 30 mm/min.

## RESULTS AND DISCUSSION

### Composite structure by XRD

Figure 3 presents the XRD patterns for the two layered zirconium compounds used as PET filler. In addition

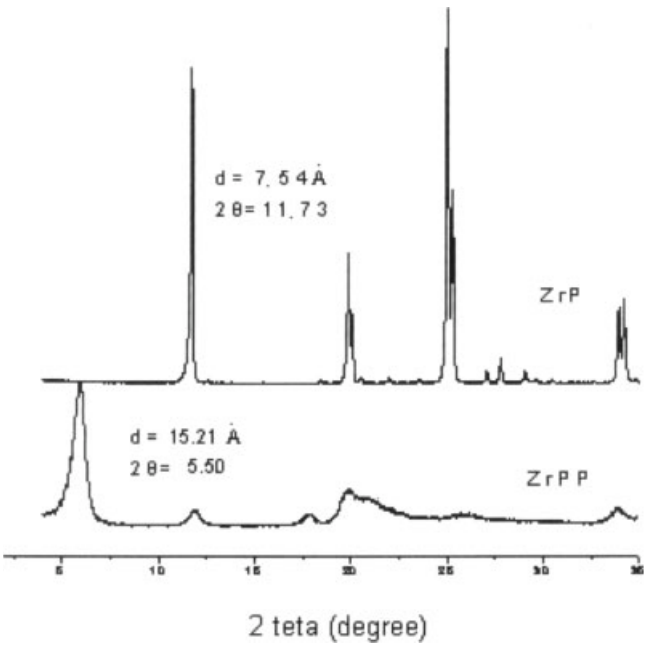


**Figure 3** XRD curves of ZrP and ZrPP crystals.

to the reflections of crystalline planes at wide angles, it shows characteristic low-angle reflections related to layered solids with a basal spacing that corresponds to interlayer distances of 7.54 Å (2θ 11.7°) for ZrP and 15.24 Å (2θ 5.5°) for ZrPP, values close to previous reports.[6,9] In contrast to ZrP, which showed thin peaks, ZrPP XRD patterns exhibit only broad ill-defined reflections, suggesting a high degree of disorder due to the presence of the large phenyl groups in the structure of the layer. This fact could help improve lamellae delamination and nanocomposite formation.

Figure 4 presents the XRD profiles of PET and PET/ZrP composites containing 2 and 5 wt % of the lamellar filler. In these profiles PET presents itself as a low crystallinity material because of the quenching effect caused during the preparation of the specimens. The low crystallinity is evidenced by a single amorphous halo in the diffraction profiles. The interlayer $d$ values for the 2 and 5 wt % ZrP in PET/ZrP composites calculated by XRD curves were 7.42 and 7.47 Å, respectively. The lower angle reflections observed for the composites appeared at a similar position of the reflection found for the α-ZrP crystal, indicating that the lamellar structure was maintained after melt processing the materials under the conditions used in the work. In fact, the crystal interlayer distances in these composites showed a small reduction when compared to the ones found in the α-ZrP crystal ($d$ = 7.54 Å) before processing. This reduction could be justified by the loss of water molecules, naturally found inside the crystal, caused by the high processing temperature.[14] Regarding this result, we concluded that the ZrP was neither intercalated by

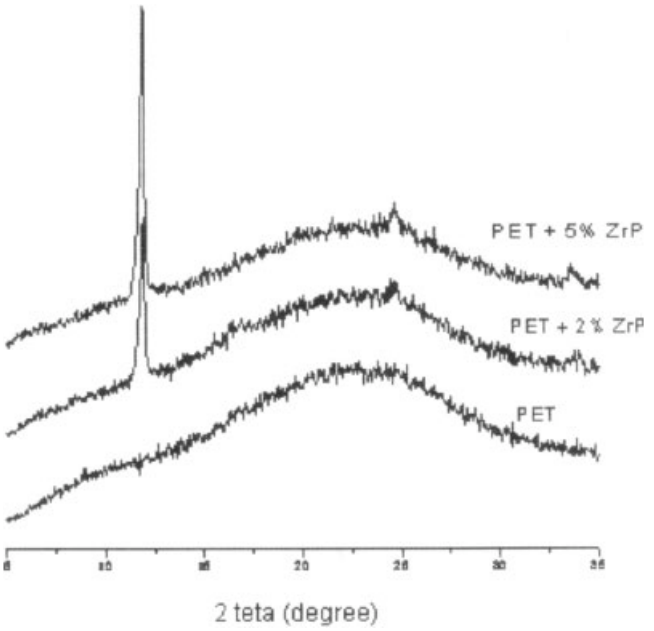


**Figure 4** XRD curves of PET and PET/ZrP composites.

PET chains nor delaminated and therefore a delaminated nanocomposite was not formed.

Figure 5 shows XRD profiles of PET and PET/ZrPP composites containing 2 and 5 wt % of the organic–inorganic hybrid phosphate filler. This figure presents XRD profiles in which the reflection at 2θ 5.5° is very weak, indicating dramatic loss of the original ZrPP lamellar crystal structure. This fact suggests that a significant change of the ZrPP original structure had taken place when the filler was processed together with PET, which suggests filler delamination or a high degree of polymer intercalation.

Comparing the response of PET/ZrP and PET/ZrPP systems, the changes observed in the XRD patterns for PET/ZrPP composites can be justified by two reasons: in the case of ZrP, layer interaction is predominantly hydrogen bonds that are stronger than the interaction of phenyl rings in ZrPP; and the higher interaction of PET phenyl rings with the pendant phenyl groups disposed between lamellar surfaces in the ZrPP crystal. Thus, it is easier for a polymer molecule to be inserted into the ZrPP layers than into ZrP ones. It seems that in the case of PET/ZrP, not only the lack of specific interaction between the platelet surface and polymer chains but also the large size of the PET molecules limit the intercalation of PET into the layered ZrP crystal structure.

## Morphology by TEM

TEM images of the PET/ZrP composite containing 5 wt % filler at two magnifications are provided in Figure 6. At lower magnification [Fig. 6(a), original magnification ×10,000] the particles appeared as well-dispersed dense spots approximately 500 nm in length isolated in a clear PET matrix. At higher magnification [Fig. 6(b), original magnification ×50,000], the image shows one single ZrP particle that, although composed of many aggregated zirconium phosphate layers, appears as a dense area with defined limits around the boundaries of the particle. The image clearly shows a pattern completely different from those presented in the literature for delaminated nanocomposites,[15] indicating that no delamination took place.

TEM images of the PET/ZrPP composite containing 5 wt % filler are presented in Figure 7. At lower magnification [Fig. 7(a), original magnification ×50,000], it is possible to see that the particles are significantly smaller than in the case of ZrP and much more dispersed than in the case of the PET/ZrP composite. Two types of particles are seen from the image: very small particles (<50 nm) of low density and the largest particles with an average size of around 200 nm formed by two regions: one of higher density and another of lower density. Figure 7(b) shows one single ZrPP particle at a higher magnification (original magnification ×100,000). The particle is significantly different in aspect than those observed in the PET/ZrP composite. In addition to a dense core, it shows a large diffuse and less dense region around the particle, suggesting that in these regions the polymer could be highly intercalated. It is important to note that total exfoliation of particles cannot be stated because the image is completely different from previous reported images of exfoliated nanocomposites.[15] From TEM and XRD it is possible to conclude that the PET/ZrPP system is a nanocomposite containing partially intercalated and fragmented filler. It is still important to emphasize that the filler particles have submicron dimensions, so both systems can be considered as nanocomposites.

In previous experiments with only one extrusion, we did not have visually homogeneous transparent composites. Thus, we adopted a two-step extrusion

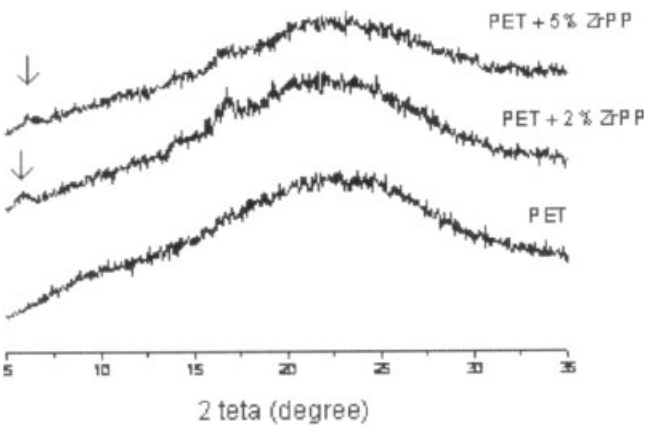


**Figure 5** XRD curves of PET and PET/ZrPP composites.

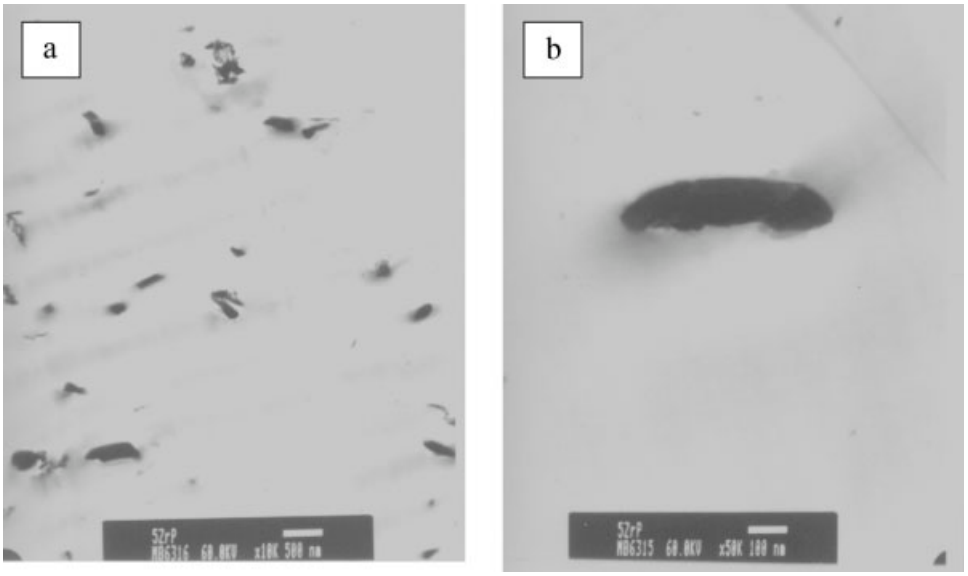


**Figure 6** TEM images of composites of PET with 5 wt % ZrP at original magnifications of (a) ×10,000 and (b) ×50,000.

method. According to our previous experience, we can improve the homogeneity of similar layered fillers such as montmorillonite by using two-step extrusion, which means an increase in residence time. In that case delamination was obtained (unpublished data) with no evidence of particle fragmentation. It is possible that, for this particular case, the increase of extrusion residence time could have increased delamination/fragmentation.

There is no previous literature reporting the fragmentation of these fillers in similar processing conditions. Because it is known that particles of both fillers are formed by primary particles (layers), it is possible that production of fragments occurs during melt processing due to shearing. It is expected that the effect of shearing is more pronounced in PET/ZrPP composites because of weaker platelet interaction.

## Thermal properties

Figures 8 and 9 present DSC traces of PET, PET/ZrP, and PET/ZrPP. Table I provides the values of glass-transition temperature ($T_g$), $T_{ch}$, $T_{cc}$, $T_m$, and $X_c$ for these materials.

DSC traces for the first heating scan of samples are shown in Figures 8(a) and 9(a). As PET, both composites present low crystallinity due to quenching that occurred on injection molding the specimens. The

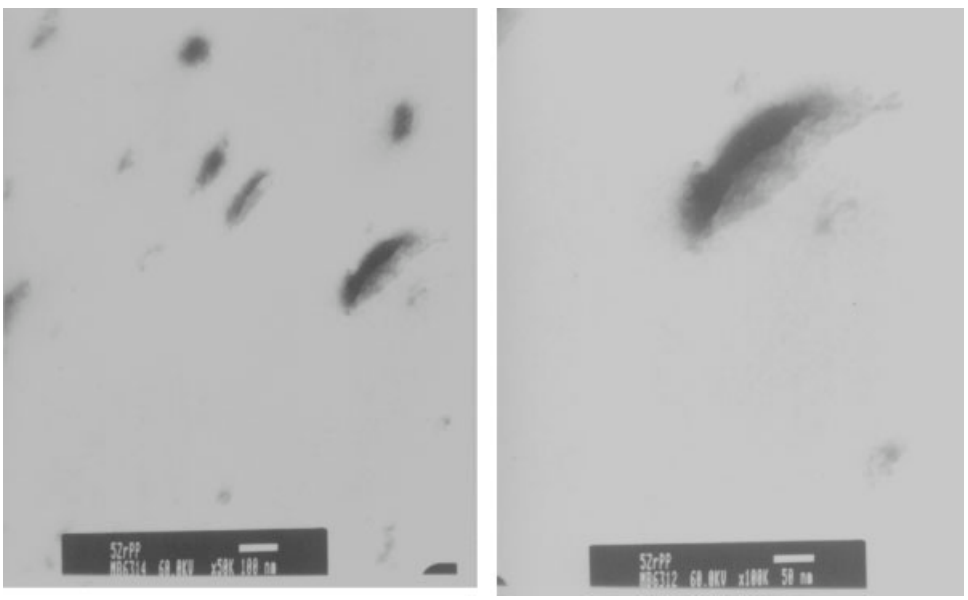

**Figure 7** TEM images of composites of PET with 5 wt % ZrPP at original magnifications of (a) ×50,000 and (b) ×100,000.

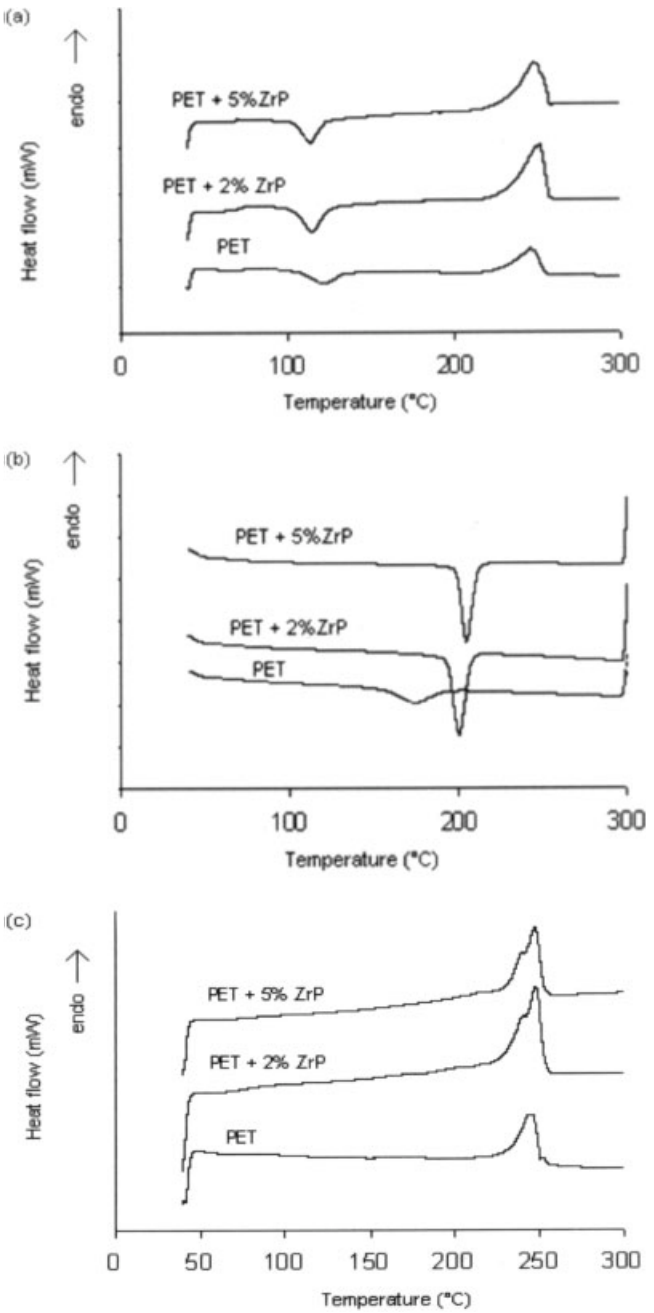


**Figure 8** DSC traces of PET and PET/ZrP composites: (a) first heating scan, (b) cooling scan, and (c) second heating.

degree of crystallinity is provided in Table I. In all cases, crystallization on heating was observed. For these composites, the $T_g$ and $T_{ch}$ showed small decreases with incorporation of the lamellar fillers. In the case of ZrPP, TEM images showing small less dense spots indicated the presence of small organic–inorganic hybrid structures in the matrix, and structures even smaller containing phenyl rings could be present, producing this $T_g$ drop. Nevertheless, the $T_g$ decrease was also observed for PET/ZrP composite, and an explanation for this behavior is not known. On this first heating, the $T_m$ did not change when the filler was added to the polyester.

During the cooling process [Figs. 8(b), (9b)], only one exothermic transition (crystallization) was observed. The $T_{cc}$ appeared at a lower temperature for PET than for PET/ZrP and PET/ZrPP, indicating that the lamellar phosphates accelerated the PET crystallization process. The increase in $T_{cc}$ indicates that the fillers affected the crystallization rate, acting as nucle-

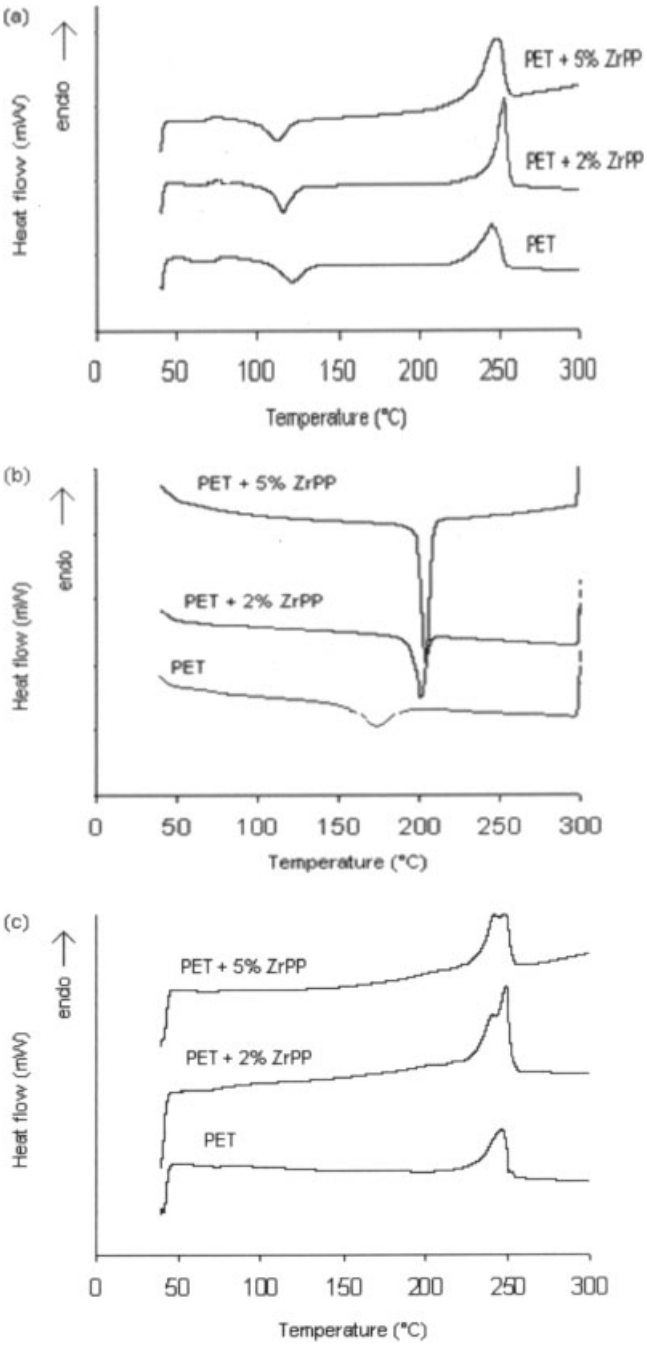


**Figure 9** DSC traces of PET and PET/ZrPP composites: (a) first heating scan, (b) cooling scan, and (c) second heating.

**TABLE I**
**Glass-Transition ($T_g$), Crystallization on Heating ($T_{ch}$), Crystallization on Cooling ($T_{cc}$), and Melting ($T_m$) Temperatures and Degree of Crystallinity ($X_c$) for PET, PET/ZrP, and PET/ZrPP**

| Sample | $T_g$ (°C) | $T_{ch}$ (°C) | $T_{cc}$ (°C) | $T_m$ (°C)[a] | $X_c$ (%)[a] | $X_c$ (%)[b] |
|---|---|---|---|---|---|---|
| PET | 75 | 121 | 174 | 246 | 14 | 31 |
| PET + 2 wt % ZrP | 69 | 115 | 201 | 248 | 18 | 36 |
| PET + 5 wt % ZrP | 67 | 114 | 204 | 248 | 20 | 39 |
| PET + 2 wt % ZrPP | 72 | 116 | 201 | 249 | 25 | 41 |
| PET + 5 wt % ZrPP | 71 | 112 | 204 | 250 | 21 | 37 |

[a] First heating run.
[b] Second heating run.

ating agents. The nucleating effect was independent of the phosphate type.

In the second heating [Figs. 8(c), (9c)], the melting temperatures showed a slight increase with filler incorporation, particularly for the PET/ZrPP sample containing 5 wt % filler. In all concentrations, the curves show double melt peaks that are probably attributable to the existence of PET crystallites having different thicknesses. A rise in the degree of crystallinity with increasing filler concentration was observed, independent of the crystal type, which is another indication of the nucleating action of the inorganic fillers on PET, in accordance with a previous report.[16] The thermal properties of PET/zirconium phosphate nanocomposites are more affected by the amount of filler than by the filler type. The influence of the organic–inorganic hybrid phosphate nanofiller on PET thermal properties was similar to that previously reported for PET–organoclay nanocomposites.[16]

Figure 10 shows weight loss curves of PET and PET/ZrPP nanocomposites obtained by TGA experiments. For comparison, TGA curves of the lamellar fillers are presented in Figure 11. The figure shows that ZrP and ZrPP are very stable materials, degrading in the range of 500–700°C. Neither material degraded at the processing temperature, suggesting that the fragmentation observed for ZrPP may be mainly due to the shearing effect. Under nitrogen, PET showed only one degradation step, leaving at about 10% residue (Fig. 10, Table II). For the PET/ZrPP thermal curves, a slight shifting of the onset temperature to a higher temperature was noted, suggesting an increase in the thermal stability of these materials. No difference in the decomposition profile was observed for PET/ZrPP nanocomposites containing 2 and 5 wt % of ZrPP. These materials left 12.6 and 15.6% residue, respectively. The enhancement of char formation was ascribed to unburned filler and the high heat resistance exerted by the filler itself.[4] This result is different from that observed for PET/montmorillonite[17] and similar to the behavior observed for nanocomposites formed by ethylene vinyl acetate and hectorite exchanged with ammonium dodecanoic acid.[18] The results observed for the PET/ZrPP system is in agreement with the literature that mentions in some cases improvement of thermal stability in highly dispersed layered materials.[2,17] Introduction of layered inorganic components into organic polymers can improve their thermal stabilities because of the heat insulation effect of the inorganic layers and the mass transport barrier to the volatile products generated during decomposition.

The results obtained for PET/ZrP composites were different from those for PET/ZrPP. TGA curves of PET/ZrP presented a small decrease in the onset temperature, which was interpreted to be attributable to the less efficient dispersion of the zirconium

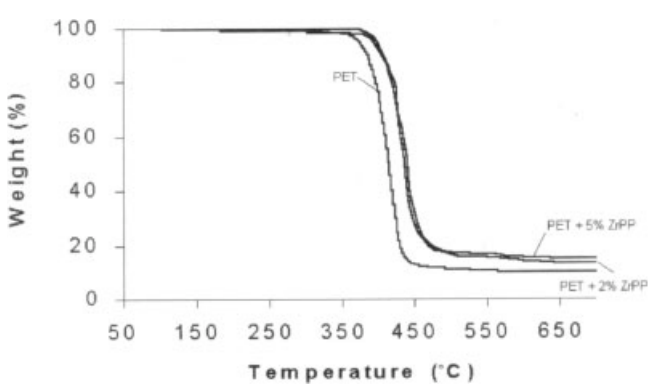


**Figure 10** TGA curves for PET and PET/ZrPP.

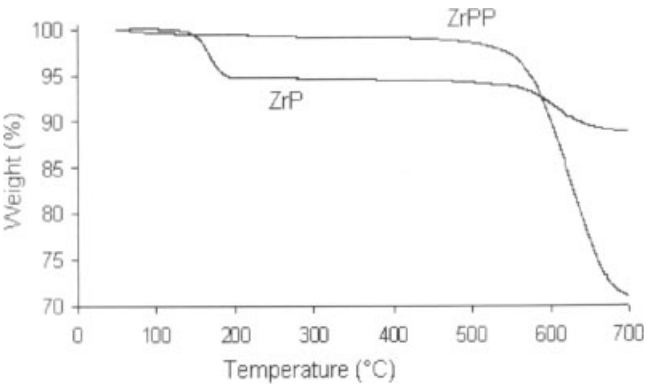


**Figure 11** TGA curves for ZrP and ZrPP crystals.

**TABLE II**
**TGA Data on Degradation of PET, PET/ZrP, and PET/ZrPP under Nitrogen**

| Sample | $T_{onset}$ (°C) | $T_f$ (°C)[a] | wt %[b] |
|---|---|---|---|
| PET | 389 | 436 | 10.2 |
| PET + 2 wt % ZrP | 358 | 408 | 11.3 |
| PET + 5 wt % ZrP | 356 | 411 | 13.1 |
| PET + 2 wt % ZrPP | 391 | 500 | 12.6 |
| PET + 5 wt % ZrPP | 394 | 515 | 15.6 |

[a] Final decomposition temperature.
[b] Residue at 700°C.

phosphate and the catalytic effect of the acidic surface of these materials. It is important to point out that, if polymer intercalation has occurred for ZrPP composites, we expect that constrained PET chains between layers would behave differently compared to PET in ZrP composites, because no intercalation is evident in that case. As is well known, acid groups can catalyze ester linkage breaks and therefore could also be another reason for the lower onset observed for ZrP composites. In conclusion, it seems that ZrP particles dispersed in the PET matrix do not interfere positively with the degradation mechanism.

### Mechanical properties

Particles in a polymer matrix can act as reinforcements as far as mechanical properties are concerned. In the layered particles, when the polymer is unable to be inserted between the lamellae, an ordinary composite is obtained. In this case, the mechanical properties settle in the same range as traditional microcomposites.[1]

Data on the mechanical properties of PET, PET/ZrP, and PET/ZrPP are presented in Table III. The tensile tests showed that the moduli increased when zirconium phosphate filler was added to PET. This increase may be ascribed to the presence of the inorganic phase and enhancement of the degree of crystallinity, induced by the filler nucleation. Nevertheless, the increase was higher for PET/ZrPP nanocomposites than for the PET/ZrP one. Therefore, the improvement in mechanical properties, usually claimed when nanocomposites are obtained, was preferentially observed in this work for PET/ZrPP systems. It is interesting to note that increases in zirconium phenylphosphonate from 2 to 5 wt % did not significantly increase the modulus. For both lamellar materials, their addition to PET decreased the elongation at break (Table III). The PET/ZrPP (2 wt %) nanocomposite presented superior elongation at break when compared to PET/ZrP. Thus, for the composite where lamellae are completely agglomerated, the material is more brittle. When the filler concentration is raised to 5 wt %, the amount of rigid elements in the material is higher, dramatically reducing the polymer yield.

The mechanical properties of these filled systems depend on two factors: the polymer matrix crystallization and the extent of filler reinforcement. Several explanations have been given about the reinforcement properties of polymer-layered particles.[3,4,19] The superior mechanical properties of these nanosystems might result from the strong interaction between the polymer molecules and layered filler.[19] Additional explanations are the decrease of spherulite dimensions and the increase of physical crosslinks with the addition of nanofiller.[20] In fact, the interactions between the lamella and the polymer at the interface form a constrained region in the vicinity of the materials layers that is due to the rigid nature of the filler.[2,21]

## CONCLUSION

Preparation of PET composites using crystalline lamellar zirconium phosphates ZrP and ZrPP were carried out by extrusion. Materials containing < 500-nm individual particles dispersed in the PET matrix were obtained. The nanocomposites formed with 2 and 5 wt % ZrPP generated XRD curves with practically an absence of low-angle reflexion at about 5.5°, indicative of loss of the original layered structure, whereas the ZrP layers of primary particles remain aggregated after the nanocomposite preparation. TEM images of ZrPP were clearly different from ZrP ones, also showing particles with dense regions that are small less dense spots indicative of particle fragmentation, which could be due to small aggregates of lamellae. In our opinion these less dense small regions were mainly constituted of organic–inorganic

**TABLE III**
**Mechanical Properties of PET, PET/ZrP, and PET/ZrPP**

| Sample | Elongation at yield (%) | Stress at yield (MPa) | Young's modulus (MPa) | Elongation at break (%) | Stress at break (MPa) |
|---|---|---|---|---|---|
| PET | 4.07 ± 0.20 | 45.34 ± 0.46 | 1582 ± 23 | 192.7 ± 21.5 | 22.1 ± 12.5 |
| PET + 2 wt % ZrP | 3.92 ± 0.04 | 46.87 ± 0.64 | 1649 ± 115 | 133.2 ± 85.5 | 19.6 ± 8.8 |
| PET + 5 wt % ZrP | 3.86 ± 0.15 | 47.08 ± 0.73 | 1779 ± 135 | 27.2 ± 21.3 | 16.7 ± 1.8 |
| PET + 2 wt % ZrPP | 3.82 ± 0.15 | 59.86 ± 0.45 | 2224 ± 145 | 174.0 ± 68.1 | 26.2 ± 9.0 |
| PET + 5 wt % ZrPP | 3.67 ± 0.08 | 58.80 ± 0.83 | 2221 ± 118 | 22.6 ± 8.0 | 22.6 ± 0.6 |

hybrid and may have been generated because of the higher interaction of phenyl groups on the lamella surface and the polymer chain. The same profile was not observed for ZrP particles. Specific interactions in the ZrPP crystal seemed to have contributed to this partial lamellar dispersion and formation of highly intercalated/partially delaminated nanocomposites. The presence of zirconium phosphate containing fillers in PET favored the increase of the polymer crystallization rate and modulus.

This work was financially supported by CNPq and FAPERJ. The authors thank the Institute of Chemistry of the Federal University of Rio de Janeiro (UFRJ) for helping with the synthesis of the lamellar phosphates and NUCAT/COPPE-UFRJ for XRD analyses.

## References

1. Alexandre, M.; Dubois, P. Mater Sci Eng 2000, 28, 1.
2. Chang, J.; Kim, S. J.; Joo, Y. L.; Im, S. Polymer 2004, 45, 919.
3. Okamoto, M.; Ray, S. S. Prog Polym Sci 2003, 28, 1539.
4. Kornmann, X. www.materials.org.br/iom/organisations/escm/newsletters4.
5. Sibele, B. C.; Pergher, A. C.; Vicente, F. Quím Nova 1999, 22, 5.
6. Clearfield, A.; Smith, G. D. Inorg Chem 1969, 8, 431.
7. Alberti, G.; Costantino, U. J Mol Catal 1984, 27, 235.
8. Alberti, G.; Costantino, U. In Intercalation Chemistry; Whittinghan, M. S.; Jacobson, A. J., Eds.; Academic: New York, 1982; p 147.
9. Alberti, G.; Costantino, U.; Alluli, S.; Tomassini, N. J Inorg Nucl Chem 1978, 40, 1113.
10. Ruiz, V. S. O.; Airoldi, C. Thermochim Acta 2004, 420, 73.
11. Clearfield, A. Prog Crystal Growth Charact 1990, 21, 1.
12. Medeiros, M. E. M.S. Thesis, University of Campinas, Campinas, Brazil, 1991.
13. Starkweather, H. W., Jr.; Zoller, P.; Jones, G. A. J Polym Sci Polym Phys Ed 1983, 21, 295.
14. Costantino, U.; Vivani, R.; Zima, V.; Cernoskova, E. J Solid State Chem 1997, 132, 17.
15. Shaha, R. K.; Hunter, D. L.; Paul, D. R. Polymer 2005, 46, 2646.
16. Vidotti, S. E.; Chinellato, A. C.; Boesel, L. F.; Pessan, L. A. J Metast Nanocryst Mater 2004, 22, 47.
17. Lewin, M. Polym Degrad Stab 2005, 88, 13.
18. Zanetti, M.; Camino, G.; Thomann, R.; Mulhaupt, R. Polymer 2001, 42, 4501.
19. Usuki, A.; Koiwai, A.; Kojima, Y.; Kawasumi, M.; Okada, A.; Kurauchi, T.; Kamigaito, O. J Appl Polym Sci 1995, 55, 119.
20. Wang, D.; Gao, J. Int J Polym Mater 2004, 53, 1085.
21. Kojima, Y.; Usuki, A.; Kawasumi, M.; Okada, A.; Fukushima, Y.; Kurauchi, T.; Kamigaito, O. J Mater Res 1993, 8, 1185.